PHYSICAL REVIEW D **71,** 016004 (2005)

Towards a relativistic description of exotic meson decays

Nikodem J. Poplawski, Adam P. Szczepaniak, and J. T. Londergan

Physics Department and Nuclear Theory Center, Indiana University, Bloomington, Indiana 47405, USA

(Received 24 August 2004; published 7 January 2005)

This work analyzes hadronic decays of exotic mesons, with a focus on the lightest one, the $J^{PC} = 1^{-+}$ π_1, in a fully relativistic formalism, and makes comparisons with nonrelativistic results. We also discuss Coulomb gauge decays of normal mesons that proceed through their hybrid components. The relativistic spin wave functions of mesons and hybrids are constructed based on unitary representations of the Lorentz group. The radial wave functions are obtained from phenomenological considerations of the mass operator. Fully relativistic results (with Wigner rotations) differ significantly from nonrelativistic ones. We also find that the decay channels $\pi_1 \rightarrow \pi b_1$, πf_1, KK_1 are favored, in agreement with results obtained using other models.

DOI: 10.1103/PhysRevD.71.016004 PACS numbers: 11.10.Ef, 12.38.Aw, 12.38.Cy, 12.38.Lg

I. INTRODUCTION

Strong hadronic decays have been a subject of phenomenological investigations for several years [1–6]. The quark model description of strong decays is based on the assumption that decays originate from creation of a quark-antiquark ($Q\bar{Q}$) pair in the gluonic field of the decaying meson. The produced $Q\bar{Q}$ pair subsequently recombines with the spectator constituents and hadronizes into the final state decay products. Such a picture is consistent with the experimental observation that most hadronic decays involve a minimal number of final state particles in the final states; this requires a small number of internal transitions at the quark level. Furthermore, the absence of complicated multiparticle hadronic decays is also consistent with a minimal analyticity assumption for the scattering amplitude. The absence of complicated multiparticle cuts in the s-channel provides justification for a simple resonance Regge pole parametrization of the t-channel amplitude over a wide s-channel energy range.

The mechanism of $Q\bar{Q}$ pair production is by itself a complicated phenomenon, which can in principle be studied through lattice gauge simulations. In the strong coupling and/or nonrelativistic limits, pair production was shown to be similar to electron-positron production in a strong uniform electric field (the Schwinger mechanism) [7]. In this case the produced $Q\bar{Q}$ pair carries the quantum numbers of the vacuum, i.e., unit spin coupled to unit relative orbital angular momentum. A phenomenological hadron decay model based on such a $Q\bar{Q}$ production mechanism is referred to as the $^3P_0$ decay model (the spectroscopic notation refers to the quantum numbers of the produced $Q\bar{Q}$ pair); this model has been extensively used in phenomenological studies of meson and baryon decays.

Within a nonrelativistic or constituent quark model Born-Oppeinhemer approach, it is assumed that formation of gluonic field distributions decouples from the dynamics of the slowly moving constituent quarks. Consequently the decay and formation of final state hadrons can be studied within a nonrelativistic quantum mechanical framework [8]. For light quarks the nonrelativistic approximation can be justified from the observation that dynamical chiral symmetry breaking leads to massive constituent quarks and transverse gluon excitations with a mass gap on the order of 1 GeV [9,10]. This heavy, effective mass of gluonic excitations results in weak mixing between the valence and multiparticle Fock sectors and suggests the validity of an approach to the decay process in which the pair production interaction is used only once.

This is also consistent with the characteristics of the experimental data on decays discussed earlier. Since fully dynamical lattice simulations of the light hadron resonances are not yet available, such a phenomenological approach seems to be a reasonable starting point towards a description of the strong decays of light hadrons.

In this paper we discuss some of the remaining issues pertaining to models based on the ideas presented above. The first issue is the question of relativistic effects. Even though a simple nonrelativistic description appears to be quite successful in predicting decay widths of resonance with masses as large as 2–3 GeV, the presence of light quarks moving with average velocities a substantial fraction of the speed of light naturally raises the question of the validity of the nonrelativistic reduction. In the case of form factors, it has been demonstrated that relativistic effects in the quark model are in general quite large [11–14]. A study of relativistic effects in light-cone quantization has also recently been performed [15]. In the absence of a fully consistent dynamical model, one could argue that these effects might somehow be mocked up by effective parameters, nevertheless if one seeks a more ''universal'' constituent quark model of hadronic properties, it is essential to address the role of relativistic corrections in decays.

Second, as discussed above since the $^3P_0$ decay model can be related to the characteristics of a Wilson loop, in a consistent description of a decay process one should consider hadrons including flux-tube degrees of freedom and the effects of flux-tube breaking [16,17]. The majority of

models of normal hadron decays do not include such effects. In those models the strong decay amplitude is determined by the quark model constituent wave function, multiplied by a form factor representing pair production that is independent of the quark distribution in the parent hadron. This would not be the case for a general string breaking mechanism.

A simple phenomenological picture of hadrons and their decays in terms of quantum mechanical wave functions emerges naturally in a fixed gauge approach. For example, in the Coulomb gauge the precursor of flux-tube dynamics, including string breaking, originates from the nonAbelian Coulomb potential, which also determines the quark wave functions [18–20]. The string couples to the $Q\bar{Q}$ pair via transverse gluon emission and absorption in the standard way. This coupling carries $^3S_1$ quantum numbers. It is interesting to investigate whether this coupling, combined with the flux-tube dynamics, is consistent with the phenomenological $^3P_0$ picture discussed above.

If one were to attempt a description of decays based on Coulomb gauge quantization, it is necessary to address the role of the hybrid quark-antiquark-gluon configurations, since these appear as intermediate states in the decay process as illustrated in Fig. 1. If such hybrid states also exist as asymptotic states they would provide an invaluable insight to the dynamics of confined gluons. In recent years, evidence has been presented that such states do indeed exist, in particular, in exotic channels that do not mix with the $Q\bar{Q}$ sector. The E852 collaboration reported a large signal (comparable to the $a_2(1320)$, D-wave resonance) in the exotic, P-wave of the $\eta'\pi^-$ channel near 1600 MeV [21,22]. A somewhat narrower state has been measured at a very similar mass decaying into $\rho\pi^-$ [23]. Both, the E852 and the Crystal Barrel collaborations reported an exotic $J^{PC} = 1^{-+}$ state in $\eta\pi$ channel with a mass close to 1400 MeV [24,25], but an analysis of the Indiana group has questioned the resonance interpretation of this signal [26]. More recent analyses of the E852 data led to reports of two $J^{PC} = 1^{-+}$ waves in $f_1(1285)\pi^-$ [27] and $b_1(1235)\pi$ [28] decay modes at $M = 1600 - 1700$ MeV and $M = 2000$ MeV. A number of experiments the near future, e.g., GlueX at JLab, COMPASS at CERN, or PANDA at GSI, will closely examine the exotic meson spectrum.

Recently the nonrelativistic $^3P_0$ decay model has been extended to study hybrid meson decay, modeled via a $Q\bar{Q}$ pair coupled to a constituent, nonrelativistic string (a ''flux-tube'') [29–32]. It is therefore desirable to compare the universal decay picture of $Q\bar{Q}$ and $Q\bar{Q}g$ mesons emerging from the Coulomb gauge, as illustrated in Fig. 1, with the exotic meson decay phenomenology based on models of flux-tube breaking.

In this paper we will investigate hybrid meson decays in a relativistic, Coulomb gauge motivated description. This is a necessary first step towards understanding the phenomenology of normal meson decays. In the following section we discuss the construction of the Coulomb wave function for mesons and exotic hybrid mesons. For exotic hybrids we concentrate on the $J^{PC} = 1^{-+}$ quantum numbers which are expected for the lightest exotic multiplets [33–36]. As more data becomes available and resonance parameters are better established our approach may be used to confront the experimental results and to provide insight into the underlying quark-gluon dynamics. Another

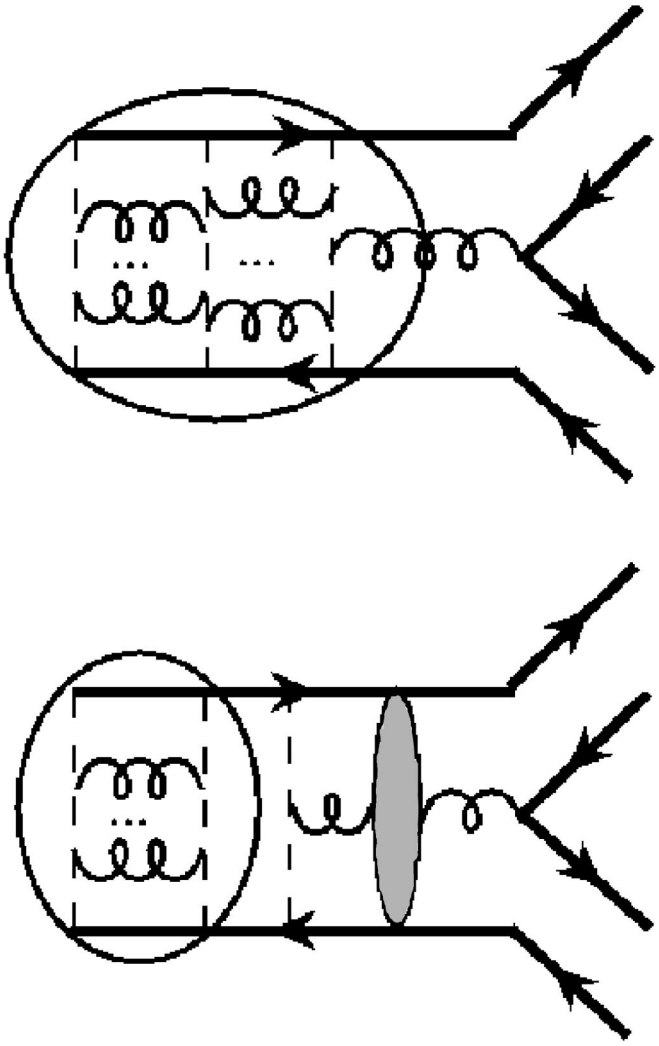

FIG. 1. Quark flow diagram responsible for strong decays of $Q\bar{Q}g$ hybrids mesons (upper) and $Q\bar{Q}$ normal mesons (lower). In the upper diagram the dashed lines represent the confining nonAbelian Coulomb potential. The gluons connecting the Coulomb lines represent formation of the flux-tube, e.g., the gluon string in the ground state. The overall state depicted is enclosed by the solid oval. Emission of a quark-antiquark pair from a gluon leads to a readjustment of the gluon strings and formation of the normal mesons in the final state. In the lower diagram the hybrid meson state appears as an intermediate state in a normal meson decay, which is assumed to proceed via mixing of a $Q\bar{Q}$ pair with virtual excitation of a gluonic string and its subsequent decay.

important contribution of this work is the step towards developing a strong decay model in a close connection with QCD, for which Coulomb gauge is the natural choice when dealing with semirelativistic systems. In Sec. III we discuss the role of relativistic effects and give numerical predictions for various decay modes. In Sec. IV we consider decays of normal mesons, in particular, the ρ and b_1. In Sec. V we summarize our results and present future plans.

II. MESON AND HYBRID WAVE FUNCTIONS

Recently lattice data has become available for static $Q\bar{Q}$ potentials with excited gluonic flux [9,10]. In Born-Oppeinhemer approximation the lightest exotic hybrids, which by definition do not mix with the ground state $Q\bar{Q}$ configuration, correspond to states built on top of the first excited adiabatic potential. The gluonic configurations can be classified according to symmetries of the $Q\bar{Q}$ system, similar to the case of a diatomic molecule. The strong interaction is invariant under rotations around the $Q\bar{Q}$ axis, reflection in a plane containing the two sources, and with respect to the product of parity and charge conjugation; thus each configuration can be labeled by the corresponding eigenvalues denoted by $\Lambda = 0, 1, \cdots$, $Y = \pm 1$, and $PC = \pm 1$ respectively. In the ground state the gluonic flux-tube has $\Lambda = 0$ and in the first excited state it has one unit of spin, $\Lambda = 1$. Furthermore in the first excited configuration, lattice simulations find $PC = -1$ for the gluon cloud [9,10,37]

In the Coulomb gauge the quantum numbers of gluonic states can be associated with those of the extra transverse gluon in the presence of a static $Q\bar{Q}$ source. This is because the transverse gluons are dressed [19,38], and on average behave as constituents with effective mass $m_g \sim 600$ MeV[39,40]. Thus low lying excited gluonic states are expected to have a small number of transverse gluons. The flux-tube itself is expected to emerge from the strong coupling of transverse gluons to the Coulomb potential. The transverse gluon wave function can be obtained by diagonalizing the net quark-antiquark-gluon interactions shown in Fig. 2 (in addition to the gluon kinetic energy).

The three-body interaction shown in Fig. 2 is of particular relevance. If the gluon is in a relative S-wave with respect to the $Q\bar{Q}$ system it has a net $PC = +1$, which is opposite to the lattice results for the first excited configuration. However, the transverse gluon has a gradient coupling to the Coulomb potential, thus a P-wave transverse gluon receives no energy shift from this coupling and the energy of the S-wave gluon state is increased. In the Coulomb gauge picture, the shift of the S-wave state via this 3-body interaction may be the cause of the inversion of $S - P$ levels seen on the lattice [41]. A quantitative analysis of this effect will be the subject of a separate investigation. In the following, when considering the wave function of an exotic hybrid we will assume that the transverse gluon is in a P-wave relative to the $Q\bar{Q}$ state.

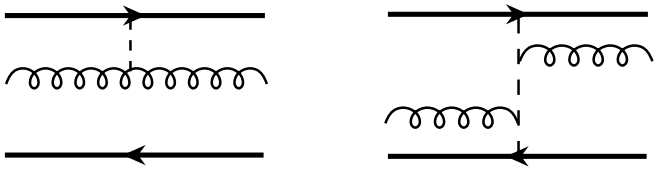

FIG. 2. Two-body (left) and three-body (right) potential between the transverse gluon and the static $Q\bar{Q}$ sources. The dashed line represents the expectation value of the nonAbelian Coulomb potential.

A. Mesons as $Q\bar{Q}$ bound states

In this analysis we do not solve the Coulomb gauge QCD Hamiltonian to obtain meson wave functions. Instead, we use the general transformation properties under the remaining kinematical symmetries (rotations and translations) to construct the states. Finally we employ Lorentz transformations as for noninteracting constituents to obtain meson wave functions for finite center of mass (c.o.m.) momenta that are required in decay calculations. This is clearly an approximation which cannot be avoided without solving the dynamical equations for the boost generators [12,13]. In the following section we examine some single particle observables to investigate this approximation.

For a system of noninteracting particles the spin wave function is constructed as an element of an irreducible, unitary representation of the Poincare group [42–46]. We will assume isospin symmetry $m_{u,d} = m$ and treat the light flavors first. The generalization to strange and heavier mesons will be given at the end of this section.

In the rest frame of a quark-antiquark pair the quark momenta are given by

$$\mathbf{l}_q^\mu = [E(m, \mathbf{q}), \mathbf{q}], \qquad l_{\bar{q}}^\mu = [E(m, -\mathbf{q}), -\mathbf{q}], \tag{1}$$

and the normalized spin-0 and spin-1 wave function corresponding to $J^{PC} = 0^{-+}$ and $J^{PC} = 1^{--}$ are given by the Clebsch-Gordan coefficients,

$$\Psi_{q\bar{q}}(\mathbf{q}, \mathbf{l}_{q\bar{q}} = 0, \sigma_q, \sigma_{\bar{q}}) = \left\langle \frac{1}{2}, \sigma_q; \frac{1}{2}, \sigma_{\bar{q}} \,\middle|\, 0, 0 \right\rangle = \frac{[i\sigma_2]_{\sigma_q \sigma_{\bar{q}}}}{\sqrt{2}} \tag{2}$$

and

$$\Psi_{q\bar{q}}^{\lambda_{q\bar{q}}}(\mathbf{q}, \mathbf{l}_{q\bar{q}} = 0, \sigma_q, \sigma_{\bar{q}}) = \left\langle \frac{1}{2}, \sigma_q; \frac{1}{2}, \sigma_{\bar{q}} \,\middle|\, 1, \lambda_{q\bar{q}} \right\rangle = = \frac{[\sigma^i i\sigma_2]_{\sigma_q \sigma_{\bar{q}}}}{\sqrt{2}} \epsilon^i(\lambda_{q\bar{q}}), \tag{3}$$

respectively. These can also be expressed in terms of Dirac spinors as

$$\Psi_{q\bar{q}}(\mathbf{q}, \mathbf{l}_{q\bar{q}} = 0, \sigma_q, \sigma_{\bar{q}}) = \frac{1}{\sqrt{2}m_{q\bar{q}}}\bar{u}(\mathbf{q}, \sigma_q)\gamma^5 v(-\mathbf{q}, \sigma_{\bar{q}}) \tag{4}$$

and

$$\Psi^{\lambda_{q\bar{q}}}_{q\bar{q}}(\mathbf{q}, \mathbf{l}_{\mathbf{q}\bar{\mathbf{q}}} = 0, \sigma_q, \sigma_{\bar{q}}) = \frac{1}{\sqrt{2}m_{q\bar{q}}}\bar{u}(\mathbf{q}, \sigma_q)\left[\gamma^i - \frac{2q^i}{m_{q\bar{q}} + 2m}\right] \times v(-\mathbf{q}, \sigma_{\bar{q}})\epsilon^i(\lambda_{q\bar{q}}), \tag{5}$$

where $m_{q\bar{q}}$ is the invariant mass of the $Q\bar{Q}$ pair, $m_{q\bar{q}} = E(m, \mathbf{q}) + E(m, -\mathbf{q}) = 2\sqrt{m^2 + \mathbf{q}^2}$, and $\epsilon^i(\lambda_{q\bar{q}})$ are the polarization vectors corresponding to spin-1 quantized along the z-axis. The boosted spin functions for mesons are summarized in Appendix A. The wave function of a $Q\bar{Q}$ system moving with a total momentum $\mathbf{l}_{q\bar{q}} = \mathbf{l}_q + \mathbf{l}_{\bar{q}} \neq 0$ is given by

$$\Psi^{\lambda_{q\bar{q}}}_{q\bar{q}}(\mathbf{q}, \mathbf{l}_{\mathrm{q\bar{q}}}, \lambda_q, \lambda_{\bar{q}}) = \sum_{\sigma_q, \sigma_{\bar{q}}} \Psi^{\lambda_{q\bar{q}}}_{q\bar{q}}(\mathbf{q}, \mathbf{l}_{\bar{q}} = 0, \sigma_q, \sigma_{\bar{q}}) \times D^{*(1/2)}_{\lambda_q\sigma_q}(\mathbf{q}, \mathbf{l}_{q\bar{q}})D^{(1/2)}_{\lambda_{\bar{q}}\sigma_{\bar{q}}}(-\mathbf{q}, \mathbf{l}_{q\bar{q}}), \tag{6}$$

where the Wigner rotation matrix $D^{(1/2)}_{\lambda\lambda'}(\mathbf{q}, \mathbf{P})$ corresponds to a boost with $\beta\gamma = \mathbf{P}/M$. One can show (see Appendix A) that the corresponding wave functions can be written in terms of covariant amplitudes,

$$\Psi_{q\bar{q}}(\mathbf{q}, \mathbf{l}_{q\bar{q}}, \lambda_q, \lambda_{\bar{q}}) = \frac{1}{\sqrt{2}m_{q\bar{q}}}\bar{u}(\mathbf{l}_q, \lambda_q)\gamma^5 v(\mathbf{l}_{\bar{q}}, \lambda_{\bar{q}}) \tag{7}$$

and

$$\Psi^{\lambda_{q\bar{q}}}_{q\bar{q}}(\mathbf{q}, \mathbf{l}_{q\bar{q}}, \lambda_q, \lambda_{\bar{q}}) = -\frac{\epsilon_\mu(\mathbf{l}_{q\bar{q}}, \lambda_{q\bar{q}})}{\sqrt{2}m_{q\bar{q}}}\bar{u}(\mathbf{l}_q, \lambda_q) \times \left[\gamma^\mu - \frac{l^\mu_q - l^\mu_{\bar{q}}}{m_{q\bar{q}} + 2m}\right]v(\mathbf{l}_{\bar{q}}, \lambda_{\bar{q}}), \tag{8}$$

where $\epsilon^\mu(\mathbf{l}_{q\bar{q}}, \lambda_{q\bar{q}})$ are obtained from $(0, \epsilon^i(\lambda_{q\bar{q}}))$ through a Lorentz boost with $\beta\gamma = \mathbf{l}_{q\bar{q}}/m_{q\bar{q}}$. Obviously $\mathbf{l}_q = \Lambda(0 \to \mathbf{l}_{q\bar{q}})\mathbf{q}$ and $\mathbf{l}_{\bar{q}} = \Lambda(0 \to \mathbf{l}_{q\bar{q}})(-\mathbf{q})$.

By coupling Eqs. (4) and (5) for $\mathbf{l}_{q\bar{q}} = 0$ with one unit of the orbital angular momentum $L = 1$ and then making the boost in Eq. (6), one obtains, respectively, the spin wave function for the quark-antiquark pair with quantum numbers $J^{PC} = 1^{+-}$,

$$\Psi^{J,\lambda_{q\bar{q}}}_{q\bar{q}} = \frac{1}{\sqrt{2}m_{q\bar{q}}(\mathbf{l}_q, \mathbf{l}_{\bar{q}})}\bar{u}(\mathbf{l}_\mathbf{q}, \lambda_q)\gamma^5 v(\mathbf{l}_{\bar{q}}, \lambda_{\bar{q}})Y_{1\lambda_{q\bar{q}}}(\bar{\mathbf{q}}), \tag{9}$$

or for $J^{PC} = 0^{++}$, 1^{++} and 2^{++},

$$\Psi^{\lambda_{q\bar{q}}}_{q\bar{q}} = -\sum_{\lambda,l}\frac{1}{\sqrt{2}m_{q\bar{q}}}\bar{u}(\mathbf{l}_q, \lambda_q)\left[\gamma^\mu - \frac{l^\mu_q - l^\mu_{\bar{q}}}{m_{q\bar{q}} + 2m}\right] \times v(\mathbf{l}_{\bar{\mathbf{q}}}, \lambda_{\bar{q}})\epsilon_\mu(\mathbf{l}_{q\bar{q}}, \lambda)Y_{1l}(\bar{\mathbf{q}})\langle 1, \lambda; 1, l|J, \lambda_{q\bar{q}}\rangle, \tag{10}$$

with $\mathbf{q} = \Lambda(\mathbf{l}_{q\bar{q}} \to 0)\mathbf{l}_q$. In order to construct meson spin wave functions for higher orbital angular momenta L between the $Q\bar{Q}$ pair one need only to replace Y_{1l} with Y_{Ll}. For consistency, we should add the constant factor Y_{00} to wave functions with $L = 0$.

Now we can proceed with the construction of meson states characterized by momentum $\mathbf{P}$, spin $\lambda_{q\bar{q}}$, and isospin I. The $\pi(I = 1)$ and $\eta(I = 0)$ states ($J^{PC} = 0^{-+}$) are constructed in terms of the annihilation and creation operators:

$$|M(\mathbf{P}, I, I_3)\rangle = \sum_{\text{all }\lambda,c,f}\int \frac{d^3\mathbf{p}_q d^3\mathbf{p}_{\bar{q}}}{(2\pi)^6 2E(m, \mathbf{p}_q)2E(m, \mathbf{p}_{\bar{q}})} \times 2[E(m_q, \mathbf{p}_q) + E(m_{\bar{q}}, \mathbf{p}_{\bar{q}})] \cdot (2\pi)^3\delta^3(\mathbf{p}_q + \mathbf{p}_{\bar{q}} - \mathbf{P})\frac{1}{N(P)}\frac{\delta_{c_q c_{\bar{q}}}}{\sqrt{3}} \times \frac{F(I, I_3)_{f_q f_{\bar{q}}}}{\sqrt{2}}\Psi_{q\bar{q}}(\mathbf{p}_q, \mathbf{p}_{\bar{q}}, \lambda_q, \lambda_{\bar{q}}) \times \psi_L[m_{q\bar{q}}(\mathbf{p}_q, \mathbf{p}_{\bar{q}})/\mu]b^\dagger_{\mathbf{p}_q\lambda_q f_q c_q}d^\dagger_{\mathbf{p}_{\bar{q}}\lambda_{\bar{q}}f_{\bar{q}}c_{\bar{q}}}|0\rangle. \tag{11}$$

In the above $\Psi_{q\bar{q}}$ is the spin-0 wave function of Eq. (7), written explicitly in terms of the momenta $\mathbf{p}_q$ and $\mathbf{p}_{\bar{q}}$ instead of the relativistic relative momentum $\mathbf{q}$ and the c.o.m. momentum $\mathbf{P} = \mathbf{l}_{q\bar{q}}$, given by

$$\mathbf{p}_q = \mathbf{q} + \frac{(\mathbf{q}\cdot\mathbf{P})\mathbf{P}}{E(m_{q\bar{q}}, \mathbf{P})[m_{q\bar{q}} + E(m_{q\bar{q}}, \mathbf{P})]} + \frac{E(m, \mathbf{q})}{m_{q\bar{q}}}\mathbf{P} \tag{12}$$

and

$$\mathbf{p}_{\bar{q}} = -\mathbf{q} - \frac{(\mathbf{q}\cdot\mathbf{P})\mathbf{P}}{E(m_{q\bar{q}}, \mathbf{P})[m_{q\bar{q}} + E(m_{q\bar{q}}, \mathbf{P})]} + \frac{E(m, \mathbf{q})}{m_{q\bar{q}}}\mathbf{P}. \tag{13}$$

In Eq. (11), c, f, and I_3 denote, respectively, the color, flavor, and third component of isospin. ψ_L represents the orbital wave function resulting from the quark-antiquark interaction that leads to a bound state (meson). We assume that this function depends only on the invariant mass $m_{q\bar{q}}$. The normalization constant N (with $P = |\mathbf{P}|$) is fixed by

$$\langle \mathbf{P}, \alpha|\mathbf{P}', \alpha'\rangle = (2\pi)^3 2E(m_M, \mathbf{P})\delta^3(\mathbf{P} - \mathbf{P}')\delta_{\alpha\alpha'}, \tag{14}$$

where m_M is the meson mass and α represents spin and isospin. The parameter μ is a scalar function of the meson quantum numbers. Finally, $F(I, I_3)$ is a 2×2 isospin matrix ($f = 1$ for u and $f = 2$ for d):

$$F(0, 0) = I, \qquad F(1, I_3) = \sigma^i \epsilon^i(I_3). \tag{15}$$

The flavor structure of the η state (as well as other isospin zero mesons) was chosen as a linear combination $\frac{1}{\sqrt{2}} \times (|u\bar{u}\rangle + |d\bar{d}\rangle)$, although in general those states are linear combinations $\cos(\phi)[|u\bar{u}\rangle + |d\bar{d}\rangle]/\sqrt{2} + \sin(\phi)|s\bar{s}\rangle$. The $|s\bar{s}\rangle$ does not contribute to the amplitude of the decay of the π_1 and therefore may be neglected in calculations, provided this amplitude is multiplied by a factor $\cos(\phi)$.

Similarly the $\rho(I = 1)$ and $\omega, \phi(I = 0)$ states ($J^{PC} = 1^{--}$) are given by Eq. (11), but instead of $\Psi_{q\bar{q}}$ in Eq. (7) one must use $\Psi^{\lambda_{q\bar{q}}}_{q\bar{q}}$ given in Eq. (8). The $b_1(I = 1)$ and $h_1(I = 0)$ states ($J^{PC} = 1^{+-}$) contain the wave function of Eq. (9). Finally, the $a(I = 1)$ and $f(I = 0)$ states ($J^{PC} = 0, 1, 2^{++}$) correspond to Eq. (10).

The above results can be straightforwardly generalized to the case where m_q and $m_{\bar{q}}$ are different, for example, to decays into mesons with one strange quark ($I = 1/2$). The spin wave function for a quark-antiquark pair in a $J^P = 0^-$ state is

$$\Psi_{q\bar{q}}(\mathbf{l}_\mathbf{q}, \mathbf{l}_{\bar{q}}, \lambda_q, \lambda_{\bar{q}}) = \frac{1}{\sqrt{2}\tilde{m}_{q\bar{q}}} \bar{u}(m_q, \mathbf{l}_q, \lambda_q)\gamma^5 v(m_{\bar{q}}, \mathbf{l}_{\bar{q}}, \lambda_{\bar{q}}), \tag{16}$$

where $\tilde{m}_{q\bar{q}} = \sqrt{m^2_{q\bar{q}} - (m_q - m_{\bar{q}})^2}$, and the K-meson states are given by Eq. (11), with an appropriate definition of the matrix F. In Eq. (11), if $\Psi_{q\bar{q}}$ in Eq. (16) is replaced by

$$\Psi^{\lambda_{q\bar{q}}}_{q\bar{q}} = -\frac{1}{\sqrt{2}\tilde{m}_{q\bar{q}}} \bar{u}(m_q, \mathbf{l}_q, \lambda_q)\left[\gamma^\mu - \frac{l^\mu_q - l^\mu_{\bar{q}}}{m_{q\bar{q}} + m_q + m_{\bar{q}}}\right] \times v(m_{\bar{q}}, \mathbf{l}_{\bar{q}}, \lambda_{\bar{q}})\epsilon_\mu(\mathbf{l}_{q\bar{q}}, \lambda_{q\bar{q}}), \tag{17}$$

then one obtains the K^*-meson states ($J^P = 1^-$). The wave functions of strange mesons with nonzero angular momentum (such as $J^P = 1^+$) can be obtained by coupling with the spherical harmonics.

So far we have treated mesons as noninteracting $Q\bar{Q}$ pairs. The interaction between a quark and an antiquark enters through the Hamiltonian $H = P^0$ and the boost generators of the Poincare group M^{0i}. It is possible to produce models of interactions for a fixed number of constituents that preserve the Poincare algebra following the prescription of Bakamjian and Thomas [42,44]. Unfortunately such a construction does not guarantee that physical observables, e.g., current matrix elements and decay amplitudes, will obey relativistic covariance. In any case one deals with phenomenological models of the quark dynamics, therefore we follow the common practice of employing a simple (Gaussian) parametrization of the orbital wave functions with one scale parameter μ related to the size of the meson,

$$\psi_L(m_{q\bar{q}}/\mu) = e^{-m^2_{q\bar{q}}/8\mu^2}. \tag{18}$$

The Gaussian ansatz is a parametrization of the wave function which encodes the information about the range of interactions and can account for the relativistic kinematics. Short-range correlations will not be properly described by such wave functions. The gaussian wave functions have also been criticized recently in the context of the large-x behavior of generalized parton distributions [47]. We studied effects of short-range correlations on other observables, e.g., form factors in [12,13] where, as expected, it was shown that such correlations become important for matrix elements involving high momentum transfers. For strong decays this is not the case, since the break up momenta are of the order of at most a few hundred MeV. In the nonrelativistic limit (where the Wigner rotation may be ignored) all the spin wave functions for regular mesons simply reduce to the Clebsch-Gordan coefficients that we started from.

B. Hybrid mesons as $Q\bar{Q}g$ bound states

As we discussed previously, in the exotic hybrid meson wave function the gluon is expected to have one unit of orbital angular momentum with respect to the $Q\bar{Q}$ pair. In the rest frame of the 3-body system, where the $Q\bar{Q}$ pair moves with momentum $-\mathbf{Q}$ and the transverse gluon with momentum $+\mathbf{Q}$, the total spin wave function of the hybrid is obtained by coupling the $Q\bar{Q}$ spin-1 wave function of Eq. (8) and the gluon wave function ($J^{PC} = 1^{--}$) to total spin $S = 0, 1, 2$ and $J^{PC} = 0^{++}, 1^{++}, 2^{++}$ states, respectively. The exotic meson wave function with $J^{PC} = 1^{-+}$ is then obtained by adding one unit of orbital angular momentum between the gluon and the $Q\bar{Q}$ pair:

$$\Psi^{\lambda_{\rm ex}}_{q\bar{q}g(S)}(\lambda_q, \lambda_{\bar{q}}, \lambda_g) = \sum_{\lambda_{q\bar{q}}, \sigma, M, l} \Psi^{\lambda_{q\bar{q}}}_{q\bar{q}}(\mathbf{q}, -\mathbf{Q}, \lambda_q, \lambda_{\bar{q}})Y_{1l}(\bar{\mathbf{Q}}) \times \langle 1, \lambda_{q\bar{q}}; 1, \sigma | S, M\rangle D^{(1)*}_{\lambda_g\sigma} \times (\bar{\mathbf{Q}})\langle S, M; 1, l | 1, \lambda_{\rm ex}\rangle. \tag{19}$$

The spin-1 rotation matrix $D^{(1)}$, representing the gluon spin wave function, relates the transverse gluon states in the helicity basis $\sigma(= \pm 1)$ to the basis described by spin λ_g quantized along a fixed z-axis. The Clebsch-Gordan coefficients and the spherical harmonic in Eq. (19) can be expressed in terms of the polarization vectors, and the action of the rotation matrix on the gluon states results in replacing $\epsilon^i(\lambda_g)$ with $\epsilon^i_c(\mathbf{Q}, \lambda_g)$, where

$$\epsilon^i_c(\mathbf{Q}, \lambda_g) = \epsilon^j(\lambda_g)(\delta^{ij} - \bar{Q}^i\bar{Q}^j). \tag{20}$$

Using the construction of spin wave functions summarized in Appendix B, the corresponding normalized wave functions are then given by

$$\Psi^{\lambda_{\rm ex}}_{q\bar{q}g(S)} = \sum_{\lambda_{q\bar{q}}} \Psi^{\lambda_{q\bar{q}}}_{q\bar{q}}(\mathbf{q}, -\mathbf{Q}, \lambda_q, \lambda_{\bar{q}}) \zeta_{(S)}(\bar{\mathbf{Q}}, \lambda_{q\bar{q}}, \lambda_g, \lambda_{\rm ex}), \tag{21}$$

where the spin states $\zeta_{(S)}$ in Eq. (21) are given by

$$\zeta_{(S=0)} = \sqrt{\frac{3}{8\pi}} [\epsilon^*(\lambda_{q\bar{q}}) \cdot \epsilon^*_c(\mathbf{Q}, \lambda_g)][\bar{\mathbf{Q}} \cdot \epsilon(\lambda_{\rm ex})], \tag{22}$$

$$\zeta_{(S=1)} = \sqrt{\frac{3}{8\pi}} [\epsilon^*(\lambda_{q\bar{q}}) \epsilon^*_c(\mathbf{Q}, \lambda_g)] \cdot [\bar{\mathbf{Q}} \epsilon(\lambda_{\rm ex})], \tag{23}$$

$$\zeta_{(S=2)} = \sqrt{\frac{27}{104\pi}} \bar{\mathbf{Q}} \cdot [\epsilon^*(\lambda_{q\bar{q}}) \otimes \epsilon^*_c(\mathbf{Q}, \lambda_g)] \cdot \epsilon(\lambda_{\rm ex}), \tag{24}$$

with $\bar{\mathbf{Q}} = \mathbf{Q}/|\mathbf{Q}|$ and $(A \otimes B)_{ij} = 2A_{(i}B_{j)} - \frac{2}{3}\delta_{ij}(\mathbf{A} \cdot \mathbf{B})$. It is easy to show $\zeta_{(2)} = 3/\sqrt{13}(\zeta_{(1)} - \frac{2}{3}\zeta_{(0)})$. The loss of linear independence is directly related to the transversity of ϵ^i_c.

The hybrid state in its rest frame is given by

$$\begin{aligned} |\pi_1(I_3, \lambda_{\rm ex})\rangle = & \sum_{{\rm all}\lambda, c, f} \frac{1}{N_{\rm ex}} \int \frac{d^3\mathbf{p}_q d^3\mathbf{p}_{\bar{q}} d^3\mathbf{Q}}{(2\pi)^9 2E_q 2E_{\bar{q}} E_g} \cdot (2\pi)^3 2 \\ & \times (E_q + E_{\bar{q}} + E_g)\delta^3(\mathbf{p}_q + \mathbf{p}_{\bar{q}} + \mathbf{Q}) \frac{\lambda^{c_g}_{c_q c_{\bar{q}}}}{2} \\ & \times \frac{\sigma^i_{f_q f_{\bar{q}}} \epsilon^i(I_3)}{\sqrt{2}} \Psi^{\lambda_{ex}}_{q\bar{q}g}(\mathbf{p}_q, \mathbf{p}_{\bar{q}}, \lambda_q, \lambda_{\bar{q}}, \lambda_g) \\ & \times \psi'_L b^\dagger_{\mathbf{p}_q \lambda_q f_q c_q} d^\dagger_{\mathbf{p}_{\bar{q}} \lambda_{\bar{q}} f_{\bar{q}} c_{\bar{q}}} a^\dagger_{\mathbf{Q} \lambda_g c_g} |0\rangle, \end{aligned} \tag{25}$$

where the spin wave function $\Psi_{q\bar{q}g}$ was given in Eq. (21) for $S = 0, 1, 2$, and the orbital wave function ψ'_L depends only on $m_{q\bar{q}}$ and the invariant mass of the three-body system, $m_{q\bar{q}g}$. Here m_g denotes the effective mass of the gluon and $E_g = E(m_g, \mathbf{Q})$, while $\lambda^{c_g}_{c_q c_{\bar{q}}}$ are the Gell-Mann matrices.

The orbital angular momentum wave function for the $Q\bar{Q}g$ system should depend only on the invariant masses $m_{q\bar{q}}$, $m_{q\bar{q}g}$, and we will again introduce an exponential function

$$\psi'_L(m_{q\bar{q}}/\mu_{ex}, m_{q\bar{q}g}/\mu'_{\rm ex}) = e^{-m^2_{q\bar{q}}/8\mu^2_{\rm ex}} \cdot e^{-m^2_{q\bar{q}g}/8\mu'^2_{\rm ex}}. \tag{26}$$

In the nonrelativistic limit only that part of the π_1 spin wave function corresponding to the $Q\bar{Q}$ pair is reduced to a Clebsch-Gordan coefficient, whereas the functions ζ given in Eqs. (22)–(24) remain unchanged.

C. Nonexotic hybrids or $Q\bar{Q}g$ components of normal mesons

As discussed in Sec. I, in Coulomb gauge the decay of a normal $Q\bar{Q}$ meson is expected to proceed via its $Q\bar{Q}g$ component with the gluon dissociating into a $Q\bar{Q}$ pair, as shown in Fig. 3. The $Q\bar{Q}g$ component of the wave function is obtained by integrating the $Q\bar{Q}$ state over the amplitude of transverse gluon emission from the Coulomb line [19], shown by the vertical dashed line in Fig. 3, which gives,

$$\begin{aligned} & \Psi_{q\bar{q}g}\left(\frac{1}{2}\mathbf{P} + \mathbf{l}, -\frac{1}{2}\mathbf{P} - \mathbf{q}, \mathbf{q} - \mathbf{l}\right) \\ & \quad = \int \frac{d^3\mathbf{k}}{(2\pi)^3} \Psi_{q\bar{q}}(\mathbf{k}) V\left(\mathbf{k} - \frac{1}{2}\mathbf{P} - \mathbf{l}, \mathbf{k} - \frac{1}{2}\mathbf{P} - \mathbf{q}\right) \\ & \qquad \times \frac{\epsilon_c(\mathbf{q} - \mathbf{l}, \lambda_g) \cdot [\mathbf{k} - \frac{1}{2}(\mathbf{P} + \mathbf{l} + \mathbf{q})]}{\sqrt{2\omega_g(\mathbf{q} - \mathbf{l})}\Delta E}. \end{aligned} \tag{27}$$

In Eq. (27) $V(p, q)$ is given by a product of the two Faddeev-Popov operators (represented by the dashed line in Fig. 3) modified by a Coulomb kernel vertex correction. The transverse gluon couples to the Coulomb line via a derivative coupling which produces the momentum dependence of the numerator. The denominator is given by the difference between the energy of the $Q\bar{Q}$ state and the energy of the $Q\bar{Q}g$ hybrid (nonexotic) state in the absence of mixing between the two [48].

The spin-orbit structure of the $Q\bar{Q}g$ component can be inferred from Eq. (27). The momentum vector in the numerator can be coupled with the spin-orbit component of the $\Psi_{q\bar{q}}$ wave function and later coupled with the $J^{PC} = 1^{--}$ transverse gluon. For example for the ρ meson the $Q\bar{Q}g$ component can be expanded in a basis of the a_0, a_1, a_2-like $Q\bar{Q}$ wave functions all having spin one and one unit of orbital angular momentum between the quark and anti-

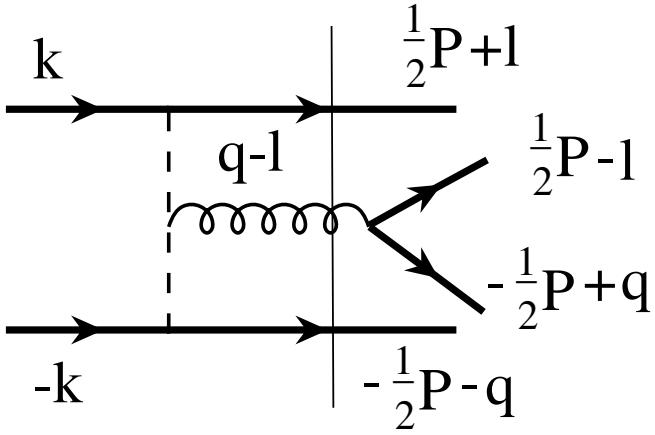

FIG. 3. Coulomb gauge description of normal meson decays. The $Q\bar{Q}$ component of the meson mixes with the $Q\bar{Q}g$ state with a subsequent decay of the transverse gluon into a $Q\bar{Q}$ pair. The vertical solid line represents the sum over all $Q\bar{Q}g$ intermediate states.

quark, coupled with the transverse gluon wave function $\epsilon_c(\mathbf{q}-\mathbf{l},\lambda_g)$ to give $J^{PC}=1^{--}$. Specifically for the ρ meson one obtains,

$$\Psi^{\lambda_\rho}_{q\bar{q}g(J)}(\lambda_q,\lambda_{\bar{q}},\lambda_g)=\sum_{\lambda_{q\bar{q}},\sigma}\Psi^{J,\lambda_{q\bar{q}}}_{q\bar{q}}(\mathbf{q},\mathbf{l}_{q\bar{q}}=-\mathbf{Q},\lambda_q,\lambda_{\bar{q}})\times D^{(1)*}_{\lambda_g\sigma}(\bar{\mathbf{Q}})\langle J,\lambda_{q\bar{q}};1,\sigma|1,\lambda_\rho\rangle. \quad (28)$$

Here $\Psi^{J,\lambda_{q\bar{q}}}_{q\bar{q}}$ are the a_0, a_1 and a_2 $Q\bar{Q}$ wave functions for $J=0,1,2$ respectively, and the gluon helicity $\sigma=\pm1$. The normalized wave functions for ρ, similar to those of π_1 in Eq. (21), are then given by

$$\Psi^{\lambda_\rho}_{q\bar{q}g(J)}=\sum_\lambda\Psi^{\lambda}_{q\bar{q}}(\mathbf{q},-\mathbf{Q},\lambda_q,\lambda_{\bar{q}})\zeta_{(J)}(\bar{\mathbf{Q}},\lambda,\lambda_g,\lambda_\rho), \quad (29)$$

where

$$\zeta_{(J=0)}=\sqrt{\frac{3}{8\pi}}[\epsilon^*(\lambda)\cdot\bar{\mathbf{q}}][\epsilon^*_c(\mathbf{Q},\lambda_g)\cdot\epsilon(\lambda_\rho)], \quad (30)$$

$$\zeta_{(J=1)}=\sqrt{\frac{9}{32\pi}}[\epsilon^*(\lambda)\times\bar{\mathbf{q}}]\cdot[\epsilon^*_c(\mathbf{Q},\lambda_g)\times\epsilon(\lambda_\rho)], \quad (31)$$

$$\zeta_{(J=2)}=\sqrt{\frac{27}{160\pi}}\epsilon^*_c(\mathbf{Q},\lambda_g)\cdot[\epsilon^*(\lambda)\otimes\bar{\mathbf{q}}]\cdot\epsilon(\lambda_\rho). \quad (32)$$

Here $\mathbf{q}$ denotes again the quark momentum in the rest frame of the $Q\bar{Q}$ pair. The most general wave function will be given by a linear combination of the three components listed above, and it can be calculated from Eq. (27).

We will also study decays of the b_1 meson which are often used as a testing ground for decay models. The $Q\bar{Q}g$ wave function with $J^{PC}=1^{+-}$, $I=1$ quantum numbers requires the $Q\bar{Q}$ to have π or π_2 quantum numbers. The corresponding total wave functions are given by

$$\Psi^{\lambda_{b_1}}_{q\bar{q}g(J)}(\lambda_q,\lambda_{\bar{q}},\lambda_g)=\sum_{\lambda_{q\bar{q}},\sigma}\Psi^{J,\lambda_{q\bar{q}}}_{q\bar{q}}(\mathbf{q},\mathbf{l}_{q\bar{q}}=-\mathbf{Q},\lambda_q,\lambda_{\bar{q}})\times D^{(1)*}_{\lambda_g\sigma}(\bar{\mathbf{Q}})\langle J,\lambda_{q\bar{q}};1,\sigma|1,\lambda_{b_1}\rangle, \quad (33)$$

with $\Psi^{J,\lambda_{q\bar{q}}}_{q\bar{q}}$ being the π (π_2) $Q\bar{Q}$ wave function for $J=0$ ($J=2$). Thus the normalized spin wave functions are given by

$$\Psi^{\lambda_{b_1}}_{q\bar{q}g(J)}=\sum_\lambda\Psi^{\lambda}_{q\bar{q}}(\mathbf{q},-\mathbf{Q},\lambda_q,\lambda_{\bar{q}})\zeta_{(J)}(\bar{\mathbf{Q}},\lambda,\lambda_g,\lambda_\rho), \quad (34)$$

where

$$\zeta_{(J=0)}=\sqrt{\frac{3}{8\pi}}[\epsilon^*_c(\mathbf{Q},\lambda_g)\cdot\epsilon(\lambda_{b_1})] \quad (35)$$

and

$$\zeta_{(J=2)}=\sqrt{\frac{27}{64\pi}}\bar{\mathbf{q}}\cdot[\epsilon^*_c(\mathbf{Q},\lambda_g)\otimes\epsilon(\lambda_{b_1})]\cdot\bar{\mathbf{q}}. \quad (36)$$

III. EXOTIC MESON DECAYS

A. Relativistic $^3S_1$ model

We assume that the transverse gluon in the π_1 creates a quark-antiquark pair and the hybrid decays into two mesons with momenta $\mathbf{P}$ and $-\mathbf{P}$. Since the quark pair is emitted in the $S=1$, $L=0$ state this decay mechanism is also referred to as the $^3S_1$ model. The Hamiltonian H of this process in Coulomb gauge is given by

$$H_{qqg}=\sum_{c,f}\int d^3\mathbf{x}\bar{\psi}_{c_1f}(\mathbf{x})[g\gamma\cdot\mathbf{A}^{c_g}(\mathbf{x})]\psi_{c_2f}(\mathbf{x})\frac{\lambda^{c_g}_{c_1c_2}}{2}. \quad (37)$$

In the constituent basis used here the single-particle quark and antiquark orbitals correspond to states of massive particles with relativistic dispersion relations, in which a running quark mass is approximated by a constant constituent mass,

$$\psi_{cf}(\mathbf{x})=\sum_\lambda\int\frac{d^3\mathbf{k}}{(2\pi)^3 2E(m,\mathbf{k})}[u(\mathbf{k},\lambda)b_{\mathbf{k}\lambda cf}+v(-\mathbf{k},\lambda)d^\dagger_{-\mathbf{k}\lambda cf}]e^{i\mathbf{k}\cdot\mathbf{x}}. \quad (38)$$

Similarly the gluon field $\mathbf{A}^{c_g}$ is expanded in a basis of transverse quasigluons, with a single-particle wave function characterizing a state of mass $m_g\sim600$ MeV,

$$\sum_\lambda\int\frac{d^3\mathbf{k}}{(2\pi)^3 2E(m_g,\mathbf{k})}[\epsilon_c(\mathbf{k},\lambda)a^{c_g}_{\mathbf{k}\lambda}+\epsilon^*_c(-\mathbf{k},\lambda)a^{\dagger c_g}_{-\mathbf{k}\lambda}]e^{i\mathbf{k}\cdot\mathbf{x}}. \quad (39)$$

In Eq. (37), g is the strong coupling constant, later chosen to be of the order 10, corresponding to $\alpha_s=O(1)$. The decay matrix element

$$\langle M_1(\mathbf{P}),M_2(-\mathbf{P})|H|\pi_1\rangle=(2\pi)^3\delta^3(\mathbf{P}-\mathbf{P})A(\mathbf{P}) \quad (40)$$

(where M denotes a meson) determines the decay amplitude A.

For decays of π_1 into $\pi\eta$ or πb_1, the spin part of the amplitude A is proportional to

$$B^{\mu j}\sum_{\lambda_g}\psi_{\mu(S)}(\mathbf{Q},\lambda_q,\lambda_{\bar{q}},\lambda_g,\lambda_{\rm ex})\epsilon^j_c(\mathbf{Q},\lambda_g), \quad (41)$$

where

$$\psi_{\mu(S)}=\sum_{\lambda_{q\bar{q}}}\zeta_{(S)}(\mathbf{Q},\lambda_{q\bar{q}},\lambda_g,\lambda_{\rm ex})\epsilon_\mu(-\mathbf{Q},\lambda_{q\bar{q}}), \quad (42)$$

and

$$B^{\mu j} = \mathrm{Tr}\Big[(\not{k} - m)(\not{p} - m)\Big(\gamma^\mu + \frac{p^\mu - l^\mu}{m_{q\bar{q}}(\mathbf{p}, \mathbf{l}) + 2m}\Big) \times (\not{l} + m)(\not{r} + m)\gamma^j \Big]. \quad (43)$$

In this expression p and l are, respectively, the four-momenta of the quark and the antiquark in the π_1, whereas r and k are the four-momenta of the quark and the antiquark created from the gluon. If $\mu_\eta = \mu_\pi$ then $A_{\pi\eta} = 0$. The 1^{-+} state is also found to have vanishing decay amplitude into two pions because of a relative minus sign from isospin that makes both terms cancel. Thus we find that the 1^{-+} isovector does not decay to identical pseudoscalars. This is a relativistic generalization of a symmetry found in other nonrelativistic decay models [30]. Since π and η are to a good approximation members of the same flavor multiplet, in the quark model one typically finds their orbital wave functions to be similar, i.e.,$\mu_\pi \sim \mu_\eta$, resulting in a small $\pi_1 \to \eta\pi$ decay rate. Of the two decay channels $\pi\eta$ and πb_1, the latter will be favored. However, the parameters μ need not be similar for two mesons with different radial quantum numbers, making corresponding channels significant. For decays of π_1 into $\pi\rho$, πf_J or ηa_J ($J = 0, 2$), the spin part is proportional to

$$C^{\mu\nu j} \sum_{\lambda_g} \psi_{\mu(S)}(\mathbf{Q}, \lambda_q, \lambda_{\bar{q}}, \lambda_g, \lambda_{\mathrm{ex}}) \epsilon_c^j(\mathbf{Q}, \lambda_g) \epsilon^{\nu *}(-\mathbf{P}, \lambda), \quad (44)$$

where λ is the spin of the second meson, and

$$C^{\mu\nu j} = \Big[(\not{p} + m)\Big(\gamma^\mu - \frac{p^\mu - l^\mu}{m_{q\bar{q}}(\mathbf{p}, \mathbf{l}) + 2m}\Big)(\not{l} - m) \times \Big(\gamma^\nu - \frac{r^\nu - l^\nu}{m_{q\bar{q}}(\mathbf{r}, \mathbf{l}) + 2m}\Big)(\not{r} + m)\gamma^j(\not{k} - m)\gamma^5 \Big]. \quad (45)$$

If $\mu_\rho = \mu_\pi$ the amplitude of the decay into $\pi\rho$ does not vanish (unlike $\pi\eta$) and this channel can be favored. The same holds for $\pi_1 \to \pi f_J$ and $\pi_1 \to \eta a_J$. For the decay $\pi_1 \to \rho\omega$, the spin part is proportional to

$$D^{\mu\nu\rho j} \sum_{\lambda_g} \psi_{\mu(S)}(\mathbf{Q}, \lambda_g) \epsilon_c^j(\mathbf{Q}, \lambda_g) \epsilon^{\nu *}(\mathbf{P}, \lambda_\rho) \epsilon^{\rho *}(-\mathbf{P}, \lambda_\omega), \quad (46)$$

where

$$D^{\mu\nu\rho j} = \mathrm{Tr}\Big[(\not{k} - m)\Big(\gamma^\nu - \frac{p^\nu - k^\nu}{m_{q\bar{q}}(\mathbf{p}, \mathbf{k}) + 2m}\Big)(\not{p} + m) \times \Big(\gamma^\mu - \frac{p^\mu - l^\mu}{m_{q\bar{q}}(\mathbf{p}, \mathbf{l}) + 2m}\Big)(\not{l} - m) \times \Big(\gamma^\rho - \frac{r^\rho - l^\rho}{m_{q\bar{q}}(\mathbf{r}, \mathbf{l}) + 2m}\Big)(\not{r} + m)\gamma^j \Big]. \quad (47)$$

If $\mu_\rho = \mu_\omega$ then $A = 0$ and the hybrid will not decay into ρ and ω. Because both parameters μ are expected to be of the same order, the channel $\pi_1 \to \rho\omega$ will not be favored.

Finally, for decays into strange mesons, one should use the above spin factors (depending on the quantum numbers), with a small modification resulting from $r^2 = k^2 = m_s^2$. The amplitudes A_{KK_1} ($S_{q\bar{q}} = 0, 1$) behave similarly to $A_{\pi b_1}$ and $A_{\pi f_1}$, whereas A_{KK^*} is like $A_{\pi\rho}$. Therefore the former will be dominant and the latter is expected to be much smaller.

The width rate for a decay into a final state with orbital angular momentum L is equal to

$$\Gamma_L = \frac{P_0}{32\pi^2 m_{\mathrm{ex}}^2} a_L^2(P_0), \quad (48)$$

where P_0 is defined by $E(m_1, \mathbf{P}_0) + E(m_2, -\mathbf{P}_0) = m_{\mathrm{ex}}$. The partial wave amplitudes are given by

$$a_L(P) = \sum_{J,\lambda,M} \int A(\mathbf{P}, \lambda_1, \lambda_2, \lambda_{\mathrm{ex}}) \times \langle J_1, \lambda_1; J_2, \lambda_2 | J, \lambda \rangle Y_{LM}(\mathbf{P}) \times \langle J, \lambda; L, M | 1, \lambda_{\mathrm{ex}} \rangle d\Omega, \quad (49)$$

with $d\Omega$ being the element of the solid angle in the direction of $\mathbf{P}$, while m and λ are, respectively, the masses and spins of the outgoing mesons.

B. Nonrelativistic limit

The nonrelativistic limit is obtained when the quark masses are large compared to the quantities μ and P_0. This is equivalent to ignoring the Wigner rotation and taking nonrelativistic phase space. In the orbital wave functions, however, we must keep next to leading order terms that depend on momenta, otherwise the amplitude would become divergent. For $\pi_1 \to \pi\eta$, πb_1 the dominant term has the form

$$B^{ij} \to -32m^4\delta^{ij} \quad (50)$$

while the other components are much smaller. Therefore the spin factor of Eq. (41) vanishes for $S = 1$, and for $S = 0$ it tends to $8\sqrt{24/\pi}m^4\bar{Q}^l\epsilon^l(\lambda_{\mathrm{ex}})$. From the above it follows $\Gamma_{(S=1)} \to 0$ and $\Gamma_{(S=2)}/\Gamma_{(S=0)} \to 4/13$. For $\pi_1 \to \pi\rho$, πf_1 we have

$$C^{ikj} \to -32im^4\epsilon^{0ikj} \quad (51)$$

and the other components are much smaller. Therefore the spin factor of Eq. (44) vanishes for $S = 0$, whereas for $S = 1$ it tends to $-8\sqrt{6/\pi}im^4\bar{Q}^i\epsilon^j(\lambda_{\mathrm{ex}})\epsilon^{k*}(\lambda)\epsilon^{ikj}$. Thus $\Gamma_{(S=0)} \to 0$ and $\Gamma_{(S=2)}/\Gamma_{(S=1)} \to 9/13$. Finally, for $\pi_1 \to \rho\omega$ we have

$$D^{ijkl} \to 32m^4(\delta^{ij}\delta^{kl} - \delta^{ik}\delta^{jl} + \delta^{il}\delta^{jk}) \quad (52)$$

(the other components are again much smaller). Therefore the spin factor of Eq. (46) tends for $S = 0$ to

$8\sqrt{24/\pi}m^4\bar{Q}^i\epsilon^i(\lambda_{ex})\epsilon^{j*}(\lambda_\rho)\epsilon^{j*}(\lambda_\omega)$, and for $S=1$ to $8\sqrt{6/\pi}m^4(\bar{Q}^i\delta^{jk}-\bar{Q}^j\delta^{ik})\epsilon^{i*}(\lambda_\rho)\epsilon^{j*}(\lambda_\omega)\epsilon^k(\lambda_{ex})$.

We can straightforwardly understand the difference in amplitudes coming from the spin wave function. If we assume $m_\eta = m_\rho$, $\mu_\eta = \mu_\rho$ and $m_{b_1} = m_{f_1} = m_{f_2}$, $\mu_{b_1} = \mu_{f_1} = \mu_{f_2}$ (the second condition for masses is satisfied to a good approximation), then one obtains

$$A_{\pi\rho} = \frac{1}{2}A_{\pi\eta} \rightarrow \Gamma_{\pi\rho} = \frac{1}{2}\Gamma_{\pi\eta} \tag{53}$$

and

$$A_{\pi f_1} = \frac{1}{2\sqrt{2}}A_{\pi b_1} \rightarrow \Gamma_{\pi f_1} = \frac{1}{8}\Gamma_{\pi b_1}, \tag{54}$$

where $A_{\pi\eta}$, $A_{\pi b_1}$ are taken for $S=0$ and $A_{\pi\rho}$, $A_{\pi f_{1,2}}$ for $S=1$. The relation between $A_{\pi\eta}$ and $A_{\pi b_1}$ (or between $A_{\pi\rho}$ and $A_{\pi f_{1,2}}$) is more complicated and depends on the orbital angular momentum wave functions ψ_L and ψ'_L. If $\mu_\rho = \mu_\pi$ then in the nonrelativistic limit π_1 will not decay into $\pi\rho$. Therefore the width for this process is expected to be much smaller than that of πb_1, assuming the parameters μ_ρ and μ_π are very close to one another. Analogous calculations can be made for the decays of π_1 into strange mesons. If $\mu_{K^*} = \mu_K$ then in the nonrelativistic limit $A_{KK^*} = 0$

C. Numerical results

Our model contains the following free parameters: the quark masses m; the effective gluon mass m_g; the size parameters μ for the wave functions; and the strong coupling constant g. The wave function parameters are constrained by the pion decay constant f_π and the elastic form factor F_π. They are, respectively, given by

$$\langle 0|A^{\mu,i}(\mathbf{0})|\pi^k(\mathbf{p})\rangle = f_\pi p^\mu \delta_{ik}, \tag{55}$$

and

$$\langle \pi^i(\mathbf{p}')|V^{\mu,j}(\mathbf{0})|\pi^k(\mathbf{p})\rangle = F_\pi(p^\mu + p'^\mu)i\epsilon_{ijk}. \tag{56}$$

The axial current $A^{\mu,i}(\mathbf{0})$ is equal to $\bar{\psi}_{cf}(\mathbf{0})\gamma^\mu\gamma_5\sigma^i\psi_{cf}/2$ and the vector current $V^{\mu,j}(\mathbf{0})$ to $\bar{\psi}_{cf}(\mathbf{0})\gamma^\mu\sigma^j\psi_{cf}/2$. By virtue of the Lorentz invariance f_π is a constant, whereas F_π is a function of $Q^2 = -(\mathbf{p}-\mathbf{p}')^2$. As was discussed previously, it is not possible to construct the currents and wave functions with a fixed number of constituents in a Lorentz covariant manner. Thus the current matrix elements are expected to violate Lorentz covariance. This will be reflected, for example, in different values of f_π obtained from spatial and time components of the axial current (rotational symmetry is not broken). Even if we replaced the factor $E(m_M, \mathbf{P})$ in Eq. (14) by 1, it would be very difficult to find generators of the Poincare group that satisfy the exact commutation relations. Thus our model with exponential orbital wave functions will not be completely invariant. The resulting form factors will depend on the frame of reference and in order to obtain $F_\pi(Q^2 = 0) = 1$ one typically employs the time component $\mu = 0$ and works in the Breit frame. For other light unflavored mesons we do not expect much variation on the ground state wave function and we choose the scale parameter μ to be of the same order as μ_π. For kaons the same procedure fits m_s and μ_K.

We will assume that the mass difference between π and ρ arises only from spin. Therefore we can write

$$m_M = \bar{m}_M + k(s_1 \cdot s_2), \tag{57}$$

where M denotes either meson and $\bar{m}_M$ is its 'averaged' mass. Substituting $m_\pi = 140$ MeV and $m_\rho = 770$ MeV we obtain $\bar{m}_M = 612$ MeV, and thus for the constituent quark masses we choose $m_u = m_d = \bar{m}_M/2 = 306$ MeV. A similar relation can be used for the K and K^* mesons, leading to $\bar{m}_K = 792$ MeV and $m_s = \bar{m}_K - m_u = 486$ MeV. The 'averaged' masses should be used in the normalization constants.

The weak decay constants can be used to fit the parameters μ_π and μ_K. Because of the Lorentz covariance breaking mentioned before, they become a function of the meson momentum and we choose them to be equal to their experimental values at rest. Thus setting $f_\pi(0) = 93$ MeV and $f_K(0) = 113$ MeV, leads to $\mu_\pi = 221$ MeV and $\mu_K = 275$ MeV. The momentum dependence of f_π in our model is presented in Fig. 4, which shows $\sim$20% difference between the value of f_π calculated for the meson at rest and for the meson with momentum approaching the light-cone. In Fig. 5 we present $F^2(Q^2)$ calculated with the wave function parameters obtained above and compared with data. There is good agreement for small momentum transfer; the discrepancy for larger Q^2 indicates the lack of sufficient high momentum components in our wave function. The strong coupling constant at this scale is approximately $g^2 = 10$, and we

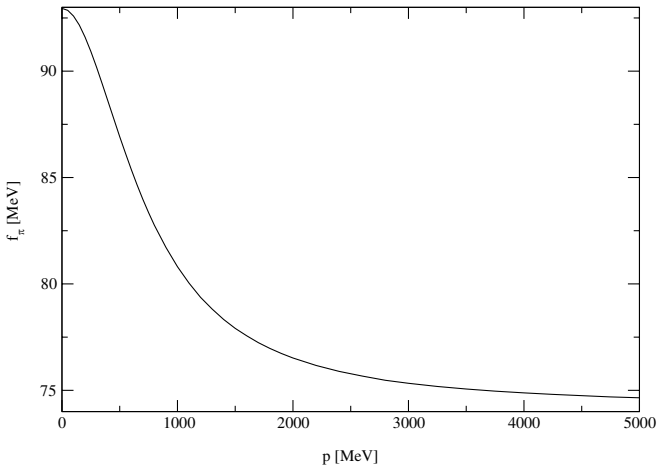

FIG. 4. The pion weak decay constant f_π as a function of the pion momentum p for $m = 306$ MeV and $\mu_\pi = 221$ MeV.

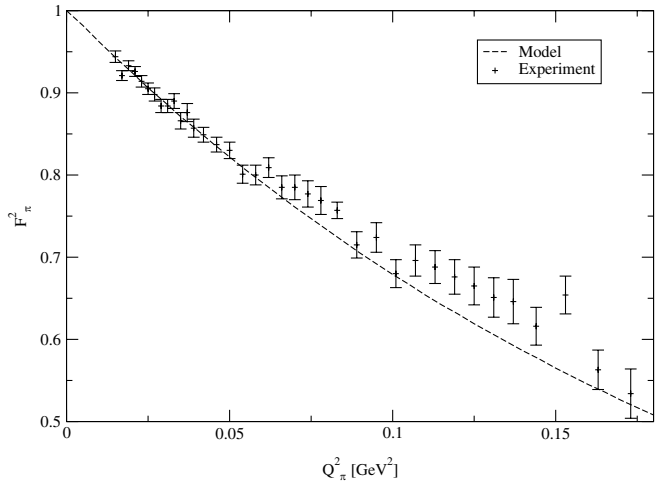

FIG. 5. The pion electromagnetic form factor F_π^2 as a function of the momentum transfer Q^2 for $m = 306$ MeV and $\mu_\pi = 221$ MeV. The experimental values are from Ref. [51].

take $m_g = 500$ MeV for the gluon effective mass. Around this value the Coulomb interaction between quark and antiquark appears to be linear.

Next we proceed to discuss relativistic effects in π_1 exotic meson decays. In Tables I and II we present the rates for various decay channels. The numbers in parentheses correspond to calculations using the nonrelativistic formulae, where S denotes the total spin of the $Q\bar{Q}g$ component of the π_1 wave function. For all unflavored mesons and the π_1, the value of the parameter μ was taken equal to μ_π, and for all strange mesons μ was set equal to μ_K. This assumption makes the widths for the channels $\pi\eta$, $\pi\eta'$ and $\rho\omega$ identically equal to zero.

In Fig. 6 we compare relativistic and nonrelativistic predictions for the width for the decay $\pi_1 \to \pi b_1$ as a function of the mass of the light quark m. It also shows the semirelativistic values, which include relativistic phase space and orbital wave functions, but no Wigner rotations.

TABLE I. Relativistic (nonrelativistic) widths in MeV for decays of the $\pi_1(1600)$. The first column gives the decay mode and the angular momentum of the corresponding partial amplitude. The three columns labeled $S = 0, 1, 2$ give the partial widths (in MeV) with S referring to the spin of the gluon-$Q\bar{Q}$ component of the exotic hybrid meson. The values in parenthesis refer to the nonrelativistic limit.

$\Gamma_{\rm rel}(\Gamma_{\rm nrel})$		$S=0$	$S=1$	$S=2$
$\pi b_1(1235)$	S	150(259)	<1(0)	44(80)
	D	<1(<1)	<1(0)	<1(<1)
$\pi f_1(1285)$	S	<1(0)	20(33)	14(23)
	D	<1(0)	<1(<1)	<1(<1)
$\pi f_2(1270)$	D	<1(0)	<1(<1)	<1(<1)
$\pi\rho(770)$	P	3(0)	<1(0)	1(0)
$KK^*(892)$	P	1(0)	<1(0)	<1(0)

TABLE II. Relativistic (nonrelativistic) widths in MeV for decays of the $\pi_1(2000)$. The labels of columns are the same as in Table I.

$\Gamma_{\rm rel}(\Gamma_{\rm nrel})$		$S=0$	$S=1$	$S=2$
$\pi b_1(1235)$	S	48(70)	<1(0)	13(22)
	D	1(2)	<1(0)	<1(<1)
$\pi f_1(1285)$	S	<1(0)	7(11)	5(8)
	D	<1(0)	2(<1)	1(<1)
$\pi f_2(1270)$	D	<1(0)	2(<1)	1(<1)
$\pi\rho$	P	2(0)	<1(0)	<1(0)
$\eta a_1(1260)$	S	<1(0)	13(22)	9(16)
	D	<1(0)	1(<1)	<1(<1)
$\eta a_2(1320)$	D	<1(0)	1(<1)	<1(<1)
$KK_1(1400)$	S	127(45)	<1(0)	39(14)
	D	<1(<1)	<1(0)	<1(<1)
$KK_1(1270)$	S	<1(0)	11(4)	7(3)
	D	<1(0)	<1(<1)	<1(<1)
$KK^*(892)$	P	1(0)	<1(0)	<1(0)

The ratios of nonrelativistic to relativistic (and semirelativistic to relativistic) values are shown in Fig. 7.

From these results it is clear that fully relativistic results are significantly different from nonrelativistic ones. There are two sources of this difference: the Wigner rotation which introduces relativistic coupling between spin and spatial degrees of freedom in the wave functions, and different relations between energy, momentum and the invariant masses (in the phase space and orbital wave functions). For realistic quark masses, both corrections appear to introduce corrections as large as 10% and thus should be included in phenomenological models.

Finally we address more quantitatively the question of reliability of the gaussian ansatz to represent the relevant component of the meson wave function participating in

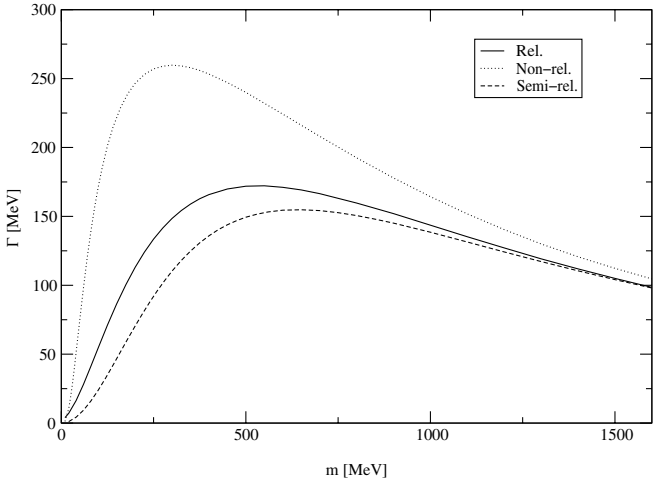

FIG. 6. Relativistic, nonrelativistic and semirelativistic widths for $\pi_1 \to \pi b_1$ in the S-wave state as a function of m, for $S = 0$ and $m_{\rm ex} = 1600$ MeV.

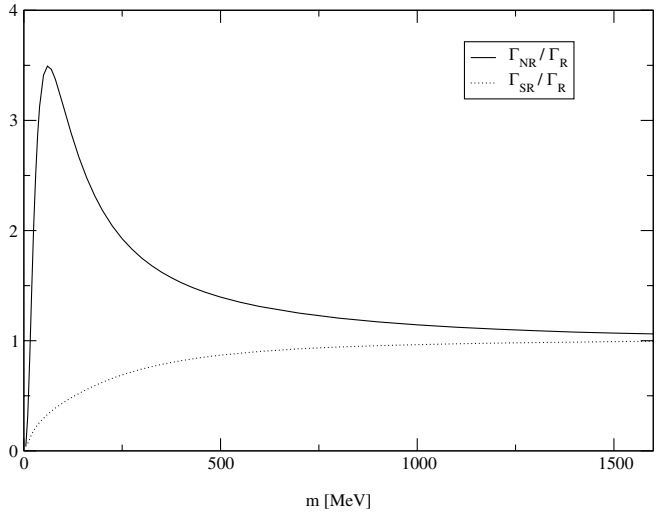

FIG. 7. Ratios of nonrelativistic to relativistic, and semirelativistic to relativistic width rates for $\pi_1 \to \pi b_1$ in the S-wave as a function of m, for $S = 0$ and $m_{\rm ex} = 1600$ MeV.

strong decays. In Fig. 8 we show the dependence of the $\pi_1(1600) \to b_1\pi$ width as a function of the gaussian size parameter (μ_{b1}) for the b_1 meson with all other parameters fixed to their values discussed above. We notice that for μ in a broad range of $150 - 400$ MeV the width changes by lest then 50%.

IV. NORMAL MESON DECAYS

In this section we will calculate the widths of the decays $\rho \to 2\pi$ and $b_1 \to \pi\omega$. These are the dominant decay channels (accounting for almost 100% of the total width) and their values are well known from experiment, and therefore can be used to test the model presented in this work.

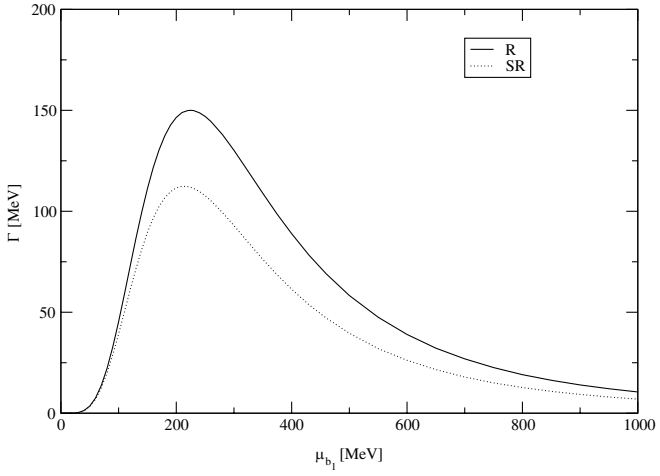

FIG. 8. Relativistic (solid line) and semirelativistic (dashed line) width for $\pi_1 \to \pi b_1$ in the S-wave state as a function of μ_{b1}, for $m_{\rm ex} = 1600$ MeV.

As discussed previously, in Coulomb gauge the decay of a normal meson is expected to proceed via $Q\bar{Q}$ mixing with the $Q\bar{Q}g$ hybrid component followed by gluon dissociation to a $Q\bar{Q}$ pair. However, the common approach to normal meson decays is based on the $^3P_0$ model where $Q\bar{Q}$ pair creation is described by an effective operator that creates the pair from the vacuum, in the presence of the normal $Q\bar{Q}$ component of the decaying meson. We will first discuss the role of relativistic effects in the $^3P_0$ model and then compare with predictions based on the Coulomb gauge picture.

A. The decay $\rho \to \pi\pi$

We start from the $^3P_0$ Hamiltonian

$$H = \Lambda \sum_{c,f} \int d^3\mathbf{x}\, \bar{\psi}_{cf}(\mathbf{x})\psi_{cf}(\mathbf{x}), \tag{58}$$

where Λ is a mass scale that can be fixed by the absolute decay width, and is expected to be of the order of the average quark momentum. In the decay matrix element the spin factor is proportional to

$$W^{\lambda_\rho} = \mathrm{Tr}\Big[(\not{k} + m)(\not{p} + m)\Big(\gamma^i - \frac{p^i - l^i}{m_{q\bar{q}}(\mathbf{p}, \mathbf{l}) + 2m}\Big) \times (\not{l} - m)(\not{r} - m)\Big]\epsilon^i(\lambda_\rho), \tag{59}$$

with the same notation used in the previous section. In the nonrelativistic limit the above expression tends to $32m^3(p^i - P^i)\epsilon^i(\lambda_\rho)$. The expression for this process is much simpler than for decays of π_1 because there is no gluon.

The decay of a ρ treated as a gluonic bound state has a similar structure to the decay $\pi_1 \to \pi\eta$, and proceeds via the $^3S_1$ interaction given by Eq. (37). The spin factor is the same as in Eq. (41) with $S = J$ and $\lambda_{\rm ex}$ replaced by λ_ρ, but the functions ζ are now given by Eqs. (30)–(32). In the nonrelativistic limit this factor will become $-8\sqrt{2/\pi}m^4\bar{q}^i\epsilon^j(\lambda_\rho)(\delta^{ij} - \bar{Q}^i\bar{Q}^j)$ for $J = 0$, $-8\sqrt{9/2\pi}m^4\bar{q}^i\epsilon^j(\lambda_\rho)(\delta^{ij} + \bar{Q}^i\bar{Q}^j)$ for $J = 1$, and $-8\sqrt{27/10\pi}m^4\bar{q}^i\epsilon^j(\lambda_\rho)\frac{1}{3}(7\delta^{ij} - \bar{Q}^i\bar{Q}^j)$ for $J = 2$. None of these functions vanishes, but only two of them remain linearly independent.

In Table III, we present numerical predictions for the widths of this decay. The experimental value of the width for $\rho \to 2\pi$ is 149 MeV. This number can be used to fit the free parameter Λ, the coupling constant g, or the hybrid scale parameter $\mu_{\rm ex'}$.

B. The decay $b_1 \to \pi\omega$

This process is a better test for the different decay schemes, because the ratio of D-wave to S-wave widths is independent of the values of Λ and g. We will begin with the picture of the b_1 as a $Q\bar{Q}$ bound state and the decay

TABLE III. Relativistic (nonrelativistic) widths in MeV for the decay $\rho(770) \to \pi\pi$ for $\Lambda = \mu_\pi$. The first column gives the prediction of the $^3P_0$ model. The three columns labeled a_0, a_1, a_2 give the predictions of the model described in this paper with spin S of the decaying gluon-$Q\bar{Q}$ component of the ρ meson equal to $S = 0, 1, 2$, respectively. The values in parenthesis refer to the nonrelativistic limit.

$\Gamma_{\rm rel}(\Gamma_{\rm nrel})$		$^3P_0$	a_0	a_1	a_2
2π	P	59(195)	7(15)	12(45)	58(75)

Hamiltonian of Eq. (58), i.e., the $^3P_0$ model. The spin factor is proportional to

$$W^{\lambda_\omega} = \mathrm{Tr}\Big[(\not{r} + m)(\not{k} - m)(\not{p} - m)(\not{l} - m) \times \left(\gamma^\mu - \frac{r^\mu - l^\mu}{m_{q\bar{q}}(\mathbf{r}, \mathbf{l}) + 2m} \right) \Big] \epsilon^*_\mu(-\mathbf{P}, \lambda_\omega), \quad (60)$$

with the same notation as for $\rho \to 2\pi$. In the nonrelativistic limit this expression tends to $32m^3(p^i - P^i)\epsilon^{i*}(\lambda_\omega)$. The spin factor for the decay of a b_1 treated as a gluonic bound state is given by Eq. (41) in which

$$B^{\mu j} = \mathrm{Tr}\Big[(\not{k} - m)(\not{p} - m)(\not{l} - m) \times \left(\gamma^\mu - \frac{r^\mu - l^\mu}{m_{q\bar{q}}(\mathbf{r}, \mathbf{l}) + 2m} \right) (\not{r} + m)\gamma^j \Big], \quad (61)$$

with $S = J$, $\lambda_{\rm ex}$ replaced by λ_{b_1}, and the functions ζ given by Eqs. (35) and (36).

The numerical predictions for the decay widths are presented in Table IV. The experimental value of the total width for the process $b_1 \to \pi\omega$ is 142 MeV, and the experimental ratio of the D-wave to S-wave widths is 0.08. Our predictions give a value less than 0.02 for this ratio in the $^3S_1$ model, and close to 1 for the $^3P_0$ decay. The real mechanism for this decay appears to lie somewhere between the two predictions. The $Q\bar{Q}g$ wave function component of the b_1 wave functions used here is that of Eq. (34), corresponding to a $Q\bar{Q}$ pair with pion quantum numbers. For a $Q\bar{Q}$ pair with π_2 quantum numbers the numerical value for the width is much smaller than 1 MeV for the S-wave and approximately 1 MeV for the D-wave. The ratio D/S is, respectively, 230. In the nonrelativistic limit one obtains similar results. It is clear that treating b_1 as $\pi_2 + g$ increases dramatically the D/S ratio; therefore this may be an important component of the wave function. The relatively small values of the decay widths of a b_1 with π_2 quantum numbers ($L = 2$) compared to those of a b_1 with pion quantum numbers ($L = 0$) remind the situation for the process $\pi_1 \to \pi b_1$, whose D-wave width was small compared to the S-wave.

TABLE IV. Relativistic (nonrelativistic) widths in MeV of the decay $b_1(1235) \to \pi\omega(782)$ for $\Lambda = \mu_\pi$. The first column gives the prediction of the $^3P_0$ model. The second column labeled π gives the predictions of the model described in this paper with the spin of the decaying gluon-$Q\bar{Q}$ component of the b_1 meson equal to $S = 0$. The values in parenthesis refer to the nonrelativistic limit.

$\Gamma_{\rm rel}(\Gamma_{\rm nrel})$		$^3P_0$	π
$\pi\omega(782)$	S	16(15)	52(82)
	D	17(42)	$<1(<1)$

V. SUMMARY AND OUTLOOK

In this work we studied relativistic effects for the decays of normal and exotic mesons, and discussed a new picture of meson decays in the Coulomb gauge point of view. In Coulomb gauge the gluon degrees of freedom are physical. Since they carry color, isolated gluons do not appear in the physical spectrum, and colorless excitations of $Q\bar{Q}g$ states are expected to be suppressed by a mass gap of the order of 1 GeV. This is what lattice QCD studies find for the energy of gluonic excitations in the presence of $Q\bar{Q}$ sources. Since strong decays are expected to proceed via gluon decay into a $Q\bar{Q}$ pair, the Coulomb gauge provides a natural framework for disentangling the dynamics of bound state formation (via a static Coulomb potential) and the decay of the gluonic component of a state.

This work led to two important conclusions. First, numerical results showed significant relativistic corrections arising from spin-orbit correlations introduced by Wigner rotation. The widths calculated using fully relativistic formulae are in general larger than the corresponding values calculated with no Wigner rotation (by a factor of roughly 10%), but smaller than completely nonrelativistic rates. Some decays that are suppressed in the nonrelativistic limit (for example $\pi_1 \to \pi\rho$ assuming identical orbital wave functions for π and ρ) acquire nonzero amplitudes in the relativistic case.

The second conclusion from this work is that the lightest exotic meson, the π_1, prefers to decay into two mesons, one of which has no orbital angular momentum while the other has $L = 1$ (the so-called $S + P$ selection rule) [30]. Thus this selection rule, also found in other models seems to be quite robust [49]. Some decays ($\pi\eta$, $\rho\omega$, KK^*) are suppressed by symmetries in orbital wave functions, or the assumption that the parameter μ should be almost equal for mesons with the same radial quantum numbers. We have also noticed that, for decays where two waves are possible, the rates for the higher partial waves are larger in the $^3P_0$ than in the $^3S_1$ model. However, there is one caveat that needs to be explored further. There are several components to the $Q\bar{Q}g$ normal meson wave functions and if there are sizable contributions from wave functions with large relative angular momentum in the $Q\bar{Q}$ system, it is possible to obtain large amplitudes for high partial waves.

This has, in particular, been illustrated in the case of the D-wave/S-wave ratio for the $b_1 \to \pi\omega$ decay.

The process $\pi_1 \to \pi\rho$ seems to be suppressed and this agrees with the $S + P$ selection rule [49]. However, some models predict larger values for its width [50]. It is possible that these are increased by the final state interactions between the outgoing mesons. The most important contribution may come from the process $\pi b_1 \to \pi\rho$, that proceeds through an ω exchange. Calculations of this contribution will be the subject of future work.

ACKNOWLEDGMENTS

The authors wish to thank J. Narebski and S. Glazek for several discussions. This work was supported in part by the U.S. Department of Energy under Contract No. DE-FG0287ER40365 and National Science Foundation Grant No. NSF-PHY0302248.

APPENDIX A: BOOSTED SPIN WAVE FUNCTIONS FOR MESONS

The polarization vectors corresponding to spin one quantized along the z-axis are given by

$$\epsilon(\pm 1) = \frac{\mp 1}{\sqrt{2}}\begin{pmatrix} 1 \\ \pm i \\ 0 \end{pmatrix}, \qquad \epsilon(0) = \begin{pmatrix} 0 \\ 0 \\ 1 \end{pmatrix}. \tag{A1}$$

The Wigner rotation matrix corresponding to a boost with $\beta\gamma = \mathbf{P}/M$ is given by

$$D^{(1/2)}_{\lambda\lambda'}(\mathbf{q}, \mathbf{P}) = \left[\frac{[E(m,\mathbf{q}) + m][E(M,\mathbf{P}) + M] + \mathbf{P}\cdot\mathbf{q} + i\sigma\cdot(\mathbf{P}\times\mathbf{q})}{\sqrt{2[E(m,\mathbf{q}) + m][E(M,\mathbf{P}) + M][E(m,\mathbf{q})E(M,\mathbf{P}) + \mathbf{P}\cdot\mathbf{q} + mM]}}\right]_{\lambda\lambda'}, \tag{A2}$$

whereas $S(\mathbf{l}_{q\bar{q}} \to 0)$ is the Dirac representation of the boost taking $\mathbf{l}_q$ to $\mathbf{q}$ and $\mathbf{l}_{\bar{q}}$ to $-\mathbf{q}$:

$$S(\mathbf{l}_{q\bar{q}} \to 0) = \frac{1}{\sqrt{2m_{q\bar{q}}[E(m_{q\bar{q}}, \mathbf{l}_{q\bar{q}}) + m_{q\bar{q}}]}} \times \begin{pmatrix} E(m_{q\bar{q}}, \mathbf{l}_{q\bar{q}}) + m_{q\bar{q}} & -\sigma\cdot\mathbf{l}_{q\bar{q}} \\ -\sigma\cdot\mathbf{l}_{q\bar{q}} & E(m_{q\bar{q}}, \mathbf{l}_{q\bar{q}}) + m_{q\bar{q}} \end{pmatrix}. \tag{A3}$$

We make use of the relations:

$$\sum_{\sigma_{\bar{q}}} D^{(1/2)}_{\lambda_{\bar{q}}\sigma_{\bar{q}}}(-\mathbf{q}, \mathbf{l}_{q\bar{q}})v(-\mathbf{q}, \sigma_{\bar{q}}) = S(\mathbf{l}_{q\bar{q}} \to 0)v(\mathbf{l}_{\bar{q}}, \lambda_{\bar{q}}), \tag{A4}$$

$$\sum_{\sigma_q} D^{*(1/2)}_{\lambda_q\sigma_q}(\mathbf{q}, \mathbf{l}_{q\bar{q}})u^\dagger(\mathbf{q}, \sigma_q) = u^\dagger(\mathbf{l}_q, \lambda_q)S^\dagger(\mathbf{l}_{q\bar{q}} \to 0), \tag{A5}$$

and the formulae:

$$S^\dagger\gamma^0 = \gamma^0 S^{-1},$$
$$S^{-1}\gamma^i S = \Lambda^i_\nu \gamma^\nu,$$
$$\epsilon_\nu(\mathbf{l}_{q\bar{q}}) = \Lambda^i_\nu(0 \to \mathbf{l}_{q\bar{q}})\epsilon_i(\lambda_{q\bar{q}}),$$

one obtains Eq. (8) from Eq. (5) and (6). One can derive the spin wave functions for other mesons in similar fashion.

APPENDIX B: SPIN WAVE FUNCTION OF THE π_1

The transverse gluon states in the helicity basis σ are related to the states in the spin basis λ_g (quantized along a fixed z-axis) by

$$|\mathbf{Q}, \lambda_g\rangle = \sum_\sigma D^{(1)*}_{\lambda_g\sigma}(\phi, \theta, -\phi)|\mathbf{Q}, \sigma\rangle, \tag{B1}$$

where θ and ϕ are, respectively, the polar angle and azimuth of the gluon momentum direction. For the gluon polarization vector we obtain

$$\epsilon^i_c(\mathbf{Q}, \lambda_g) = \sum_{\sigma=\pm 1} D^{(1)*}_{\lambda_g\sigma}(\phi, \theta, -\phi)\epsilon^i_h(\mathbf{Q}, \sigma), \tag{B2}$$

where the helicity polarization vectors are given by

$$\epsilon^i_h(\mathbf{Q}, \sigma) = \sum_{\lambda_g} D^{(1)}_{\lambda_g\sigma}(\phi, \theta, -\phi)\epsilon^i(\lambda_g). \tag{B3}$$

Using the unitarity of the matrix $D^{(1)}$ one can show

$$\epsilon^i_c(\mathbf{Q}, \lambda_g)\epsilon^{*i}_h(\mathbf{Q}, \sigma) = D^{(1)*}_{\lambda_g\sigma}(\bar{\mathbf{Q}}), \tag{B4}$$

and with the help of the identity

$$\epsilon^{*i}_h(\mathbf{Q}, \sigma)\epsilon^j_h(\mathbf{Q}, \sigma) = \delta^{ij} - \bar{Q}^i\bar{Q}^j$$

we arrive at the result:

$$\epsilon^i_c(\mathbf{Q}, \lambda_g) = \epsilon^j(\lambda_g)(\delta^{ij} - \bar{Q}^i\bar{Q}^j), \tag{B5}$$

where $\bar{\mathbf{Q}}^i = \mathbf{Q}^i/|\mathbf{Q}|$.

The Clebsch-Gordan coefficients and the spherical harmonic in Eq. (19) can be expressed in terms of the polarization vectors (A1), for example:

$$\langle 1, \lambda'; 0, 0|1, \lambda\rangle = \epsilon^*(\lambda')\cdot\epsilon(\lambda), \tag{B6}$$

$$\langle 1, \lambda'; 1, \lambda | 0, 0\rangle = \epsilon^*(\lambda') \cdot \epsilon^*(\lambda), \tag{B7}$$

$$\langle 1, \lambda'; 1, \lambda'' | 1, \lambda\rangle = \frac{i}{\sqrt{2}}[\epsilon^*(\lambda') \times \epsilon^*(\lambda'')] \cdot \epsilon(\lambda), \tag{B8}$$

$$Y_{1l}(\bar{\mathbf{Q}}) = \sqrt{\frac{3}{4\pi}}\epsilon(l) \cdot \bar{\mathbf{Q}}. \tag{B9}$$

Therefore we obtain:

$$\sum_l \langle 1, \lambda_{q\bar{q}}; 1, \lambda_g | 0, 0\rangle Y_{1l}(\bar{\mathbf{Q}}) \langle 0, 0; 1, l | 1, \lambda_{\rm ex}\rangle = [\epsilon^*(\lambda_{q\bar{q}}) \cdot \epsilon^*(\lambda_g)][\bar{\mathbf{Q}} \cdot \epsilon(\lambda_{\rm ex})], \tag{B10}$$

$$\sum_{l,s} \langle 1, \lambda_{q\bar{q}}; 1, \lambda_g | 1, s\rangle Y_{1l}(\bar{\mathbf{Q}}) \langle 1, s; 1, l | 1, \lambda_{\rm ex}\rangle = [\epsilon^*(\lambda_{q\bar{q}}) \times \epsilon^*(\lambda_g)] \cdot [\bar{\mathbf{Q}} \times \epsilon(\lambda_{\rm ex})], \tag{B11}$$

$$\sum_{l,s} \langle 1, \lambda_{q\bar{q}}; 1, \lambda_g | 2, s\rangle Y_{1l}(\bar{\mathbf{Q}}) \langle 2, s; 1, l | 1, \lambda_{\rm ex}\rangle = \bar{\mathbf{Q}} \cdot [\epsilon^*(\lambda_{q\bar{q}}) \otimes \epsilon^*(\lambda_g)] \cdot \epsilon(\lambda_{\rm ex}). \tag{B12}$$

The action of the rotation matrix $D^{(1)}$ on the gluon states results in replacing $\epsilon^i(\lambda_g)$ with $\epsilon^i_c(\mathbf{Q}, \lambda_g)$ and that leads to the spin wave functions given in Eqs. (22)–(24).

[1] A. Le Yaouanc, L. Oliver, O. Péne, and J. C. Raynal, Phys. Rev. D **8**, 2223 (1973).
[2] S. Godfrey and N. Isgur, Phys. Rev. D **32**, 189 (1985).
[3] S. Capstick and N. Isgur, Phys. Rev. D **34**, 2809 (1986).
[4] T. Barnes, F. E. Close, P. R. Page, and E. S. Swanson, Phys. Rev. D **55**, 4157 (1997).
[5] T. Barnes, N. Black, and P. R. Page, Phys. Rev. D **68**, 054014 (2003).
[6] S. Capstick and W. Roberts, Phys. Rev. D **49**, 4570 (1994); Prog. Part. Nucl. Phys. **45**, S241 (2000).
[7] H. G. Dosch and D. Gromes, Phys. Rev. D **33**, 1378 (1986).
[8] A. Le Yaouanc, L. Oliver, O. Pene, and J.-C. Raynal, *Hadron transitions in the quark model* (Gordon and Breach, New York, 1988).
[9] K. J. Juge, J. Kuti, and C. J. Morningstar, Nucl. Phys. B, Proc. Suppl. **63**, 326 (1998).
[10] K. J. Juge, J. Kuti, and C. J. Morningstar, Phys. Rev. Lett. **82**, 4400 (1999).
[11] P. L. Chung and F. Coester, Phys. Rev. D **44**, 229 (1991).
[12] A. Szczepaniak, C. R. Ji, and S. R. Cotanch, Phys. Rev. C **52**, 2738 (1995).
[13] A. Szczepaniak, C. R. Ji, and S. R. Cotanch, Phys. Rev. D **52**, 5284 (1995).
[14] B. Julia-Diaz, D. O. Riska, and F. Coester, Phys. Rev. C **69**, 035212 (2004).
[15] S. D. Glazek and A. P. Szczepaniak, Phys. Rev. D **67**, 034019 (2003).
[16] N. Isgur and J. Paton, Phys. Rev. D **31**, 2910 (1985).
[17] N. Isgur and J. Paton, Phys. Lett. **124B**, 247 (1983).
[18] A. P. Szczepaniak and E. S. Swanson, Phys. Rev. D **55**, 3987 (1997).
[19] A. P. Szczepaniak and E. S. Swanson, Phys. Rev. D **65**, 025012 (2002).
[20] P. O. Bowman and A. P. Szczepaniak, Phys. Rev. D **70**, 016002 (2004).
[21] E852 Collaboration, E. I. Ivanov *et al.*, Phys. Rev. Lett. **86**, 3977 (2001).
[22] A. P. Szczepaniak, M. Swat, A. R. Dzierba, and S. Teige, Phys. Rev. Lett. **91**, 092002 (2003).
[23] E852 Collaboration, G. S. Adams *et al.*, Phys. Rev. Lett. **81**, 5760 (1998).
[24] E852 Collaboration, S. U. Chung *et al.*, Phys. Rev. D **60**, 092001 (1999).
[25] A. Abele *et al.* Phys. Lett. B **423**, 175 (1998).
[26] A. R. Dzierba *et al.*, Phys. Rev. D **67**, 094015 (2003).
[27] E852 Collaboration, J. Kuhn *et al.*, Phys. Lett. B **595**, 109 (2004).
[28] E852 Collaboration, M. Lu *et al.*, hep-ex/0405044.
[29] R. Kokoski and N. Isgur, Phys. Rev. D **35**, 907 (1987).
[30] F. E. Close and P. R. Page, Nucl. Phys. **B443**, 233 (1995).
[31] E. S. Swanson and A. P. Szczepaniak, Phys. Rev. D **56**, 5692 (1997).
[32] P. R. Page, E. S. Swanson, and A. P. Szczepaniak, Phys. Rev. D **59**, 034016 (1999).
[33] C. Bernard *et al.*, Phys. Rev. D **68**, 074505 (2003).
[34] UKQCD Collaboration, T. Manke, I. T. Drummond, R. R. Horgan, and H. P. Shanahan, Phys. Rev. D **57**, 3829 (1998).
[35] MILC Collaboration, C. W. Bernard *et al.*, Phys. Rev. D **56**, 7039 (1997).
[36] UKQCD Collaboration, P. Lacock, C. Michael, P. Boyle, and P. Rowland, Phys. Lett. B **401**, 308 (1997).
[37] E. S. Swanson and A. P. Szczepaniak, Phys. Rev. D **59**, 014035 (1999).
[38] C. Feuchter and H. Reinhardt, hep-th/0402106.
[39] A. P. Szczepaniak and E. S. Swanson, Phys. Lett. B **577**, 61 (2003).
[40] A. P. Szczepaniak and E. S. Swanson, Phys. Rev. D **62**, 094027 (2000).
[41] A. P. Szczepaniak, Workshop on Future Directions in Quark Nuclear Physics, Adelaide, Australia, 10-20 Mar 1998 (unpublished).
[42] S. Gartenhaus and C. Schwartz, Phys. Rev. **108**, 842 (1957).
[43] R. A. Krajcik and L. L. Foldy, Phys. Rev. D **10**, 1777 (1974).
[44] B. Bakamjian and L. H. Thomas, Phys. Rev. **92**, 1300 (1953).
[45] B. L. G. Bakker, L. A. Kondratyuk, and M. V. Terent'ev,

Nucl. Phys. **B158**, 497 (1979).
[46] L. A. Kondratyuk and M. V. Terent'ev, Sov. J. Nucl. Phys. **31**, 561 (1979).
[47] M. Burkardt, Phys. Lett. B **595**, 245 (2004).
[48] A. P. Szczepaniak and P. Krupinski, Phys. Rev. D **66**, 096006 (2002).
[49] N. Isgur, R. Kokoski, and J. Paton, Phys. Rev. Lett. **54**, 869 (1985).
[50] F. E. Close and J. J. Dudek, Phys. Rev. D **70**, 094015 (2004).
[51] NA7 Collaboration, S. R. Amendolia *et al.*, Nucl. Phys. **B277**, 168 (1986).